Report

Current Biology

Towering behavior and collective dispersal in *Caenorhabditis* nematodes

Graphical abstract

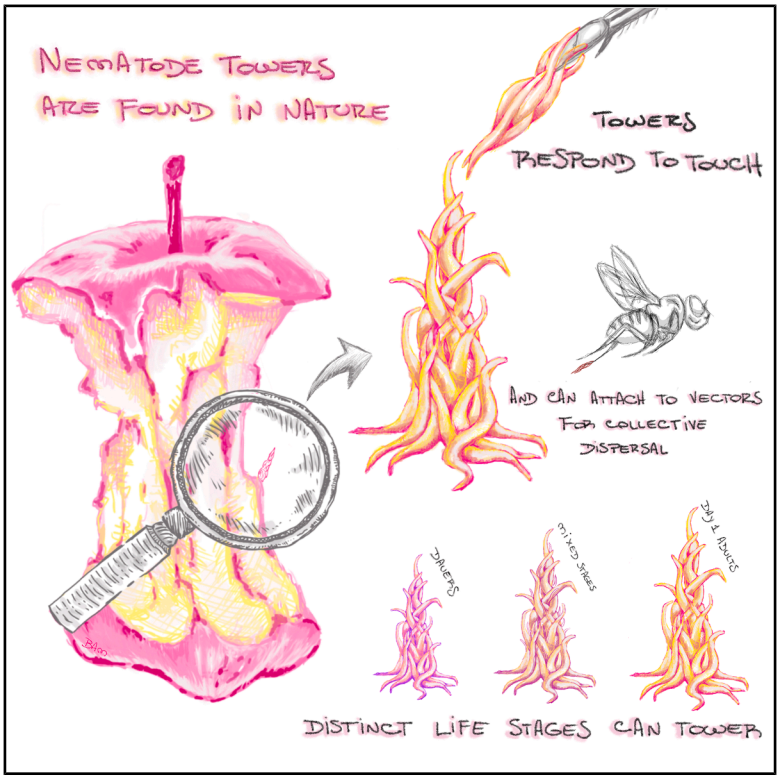

Authors

Daniela M. Perez, Ryan Greenway, Thomas Stier, Narcís Font-Massot, Assaf Pertzelan, Siyu Serena Ding

Correspondence

serena.ding@ab.mpg.de

In brief

Perez et al. report that self-assembling nematode towers occur in nature and can function as collective dispersal structures. Using *Caenorhabditis elegans*, they establish a tractable empirical model to further study the mechanism and evolution of collective dispersal behavior.

Highlights

- We report the first direct evidence of nematode towers occurring in nature
- Towers can serve to bridge gaps and disperse multiple individuals via phoresy
- Worms from all life stages can tower
- There is no role specialization among individuals in towers

Perez et al., 2025, Current Biology *35*, 2980–2986
June 23, 2025 © 2025 The Author(s). Published by Elsevier Inc.
https://doi.org/10.1016/j.cub.2025.05.026

CellPress
OPEN ACCESS

Current Biology

Report

Towering behavior and collective dispersal in *Caenorhabditis* nematodes

Daniela M. Perez,[1,2] Ryan Greenway,[1] Thomas Stier,[1,3] Narcís Font-Massot,[1,2] Assaf Pertzelan,[1] and Siyu Serena Ding[1,2,3,4,*]

[1]Max Planck Institute of Animal Behavior, Universitätsstraße 10, 78464 Konstanz, Germany
[2]Centre for the Advanced Study of Collective Behaviour, Universitätsstraße 10, 78464 Konstanz, Germany
[3]Study Program at Department of Biology, University of Konstanz, Universitätsstraße 10, 78464 Konstanz, Germany
[4]Lead contact
*Correspondence: serena.ding@ab.mpg.de
https://doi.org/10.1016/j.cub.2025.05.026

SUMMARY

Dispersal behavior allows organisms to find new resources under harsh conditions[1–5]; collective dispersal in group-living organisms raises interesting questions about kin selection, cooperation, and social conflicts that offer an exciting window into the evolution of sociality.[3,5] One type of collective dispersal is when individuals physically link their bodies into a super-organism and move as a group, but these phenomena are rare in nature and few empirical systems exist to enable their mechanistic dissection.[6–11] Individuals of many nematode species can group together and self-assemble into a living tower of worms, which is hypothesized to be a collective dispersal structure.[12–16] However, direct evidence demonstrating the occurrence and the function of towers in nature has been scarce. We documented towering behavior under natural, semi-natural, and laboratory conditions to confirm its existence and then manipulated these towers to confirm that they can bridge gaps and respond to external stimuli to confer group dispersal by phoresy. Having established the ecological and functional relevance of nematode towers, we developed a laboratory towering assay with the model organism *Caenorhabditis elegans* to exploit its experimental capabilities. Our lab assay rapidly and robustly induces towering and reveals several fundamental characteristics of both the towers and the constituent individuals, which together demonstrate the high experimental potential of using our model and the ample future research avenues that it opens. In summary, combining ecological relevance and empirical possibilities, our work sets the key foundations to establish nematode towering behavior as a powerful opportunity to elucidate the ecology, the mechanisms, and the evolution of collective dispersal.

RESULTS AND DISCUSSION

Here, we report the first evidence of nematode towers occurring in nature without any artificial interference, as all previous observations have come from semi-natural and laboratory environments.[12–15,17–19] Dispersal is important for free-living nematodes that colonize ephemeral resources,[20,21] and we conducted extensive field observations of rotting plant material around the University of Konstanz (Germany) during late summer and autumn months to establish the ecological context for nematode tower formation under natural conditions. Using a digital microscope positioned directly above undisturbed substrates, we observed towers of an undescribed *Caenorhabditis* species (*C*. sp. 8; $n = 44$)[22,23] and *C. remanei* ($n = 8$) within the damp flesh of apples and pears. As these fruits rotted and partially split on the ground, they exposed substrate projections—crystalized sugars and protruding flesh—which served as bases for towers as well as for a large number of worms individually lifting their bodies to wave in the air (nictation). All towering and nictating individuals were dauers, the stress-resistant main life stage for dispersal,[24,25] although adult nematodes were also observed crawling and feeding nearby. We observed that towers wiggle in the air together as a bundle on substrate edges and projections, analogous to nictating individuals (Figure 1A [*C*. sp. 8, dauers], Video S1). This confirmed that, as in nictation, non-planar environmental features are essential for triggering 3D towering behavior in nematodes.[17,26,27] By transferring entire towers to 55 mm Petri dishes seeded with *E. coli* OP50, we confirmed that each tower was exclusively composed of dauers from a single species ($n = 52$ towers, mean = 27.7 ± 30.6, median = 14.5 individuals per tower), despite the presence of multiple species of nematodes at various life stages on the same piece of fruit. Our additional observations on a mushroom farm in North Berwick, UK,[28] confirmed that dauers of the model organism species *C. elegans* also towered under semi-natural conditions (Figure 1B).

Towers can respond to touch for active attachment[13] and potentially allow for the collective transport of individuals,[14] although direct evidence for the putative function of towering behavior was lacking. The natural towers responded to tactile stimuli in the field (Video S1), and we frequently observed towers co-occurring on fruits with dipteran and coleopteran adults and larvae. Thus, we tested whether insects can serve as vectors for transferring towers, a frequently evoked hypothesis and true of

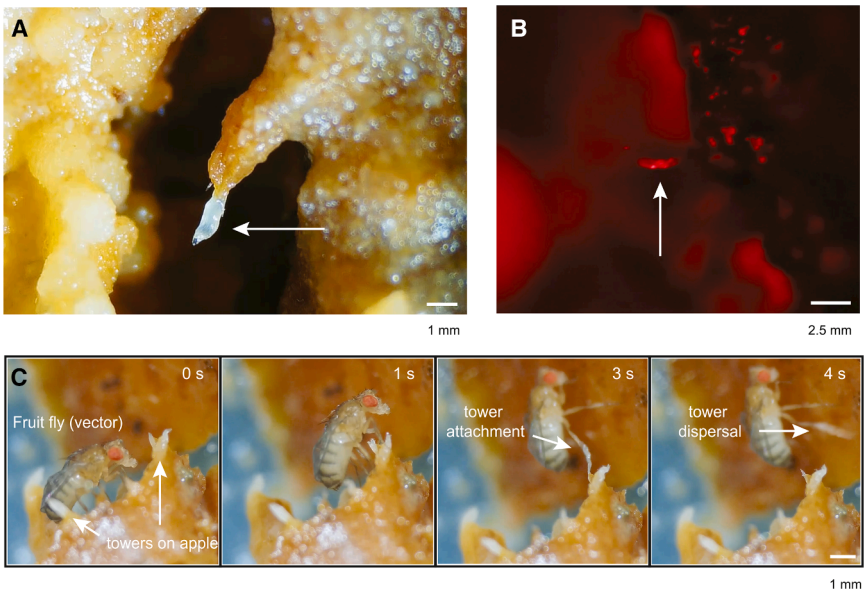

Figure 1. Nematode towers under natural and semi-natural conditions

Snapshots from videos showing: (A) a natural dauer tower (*Caenorhabditis* sp. 8) on a rotting pear in the wild (Video S1); (B) a tower on mushroom growth compost on a farm, where samples consisted mostly of dauer animals (*C. elegans*); and (C) phoretic behavior of a dauer tower (*C.* sp. 8) on a rotting apple in the Petri dish using *Drosophila melanogaster* as a vector (Video S1).

nictating individual dauers for *Caenorhabditis* species.[17,29,30] After introducing adult *Drosophila melanogaster* onto Petri dishes containing nematode towers from wild collected apples, we observed that towers are capable of detaching from the substrate and attaching to flies as they walk by (n = 2; Figure 1C [*C.* sp. 8, dauers], Video S1). We also observed that these towers were able to grow tall enough to bridge an air gap to reach a new surface above (Video S1).

Our observations of nematode towering in the wild provide the missing link to showcase this behavior as a novel model for investigating collective dispersal behavior. To establish towering's experimental potential, we promoted towers in replicable and controlled conditions using lab-cultured *C. elegans* for all subsequent laboratory experiments to exploit its experimental capacity. We developed a laboratory assay that induces towering behavior with higher experimental control than previous methods,[14,17,26] and identified that a high density of individuals, the absence of nutrients, and the presence of a climbing structure are three key conditions for promoting towering in the lab. We placed approximately 4,000 worms (*C. elegans* strains N2, CB4856, or OMG8) in a dense droplet in a 35-mm nutrient-free Petri dish filled with 2% agar (no towering occurs in the presence of bacterial food, Figure S1A), at the base of a single toothbrush bristle (hereafter referred to as a "pillar") planted on the agar as a reproducible climbing structure for the worms (Figures 2A–2C [CB4856, various life stages], Video S2). The pillar offered sufficient support for towers but with low enough friction such that worms could not easily reach the top as isolated individuals. Whereas a previous assay for inducing dauer "swarming" (similar to nematode towers) using standard pipette tips takes days and requires larger populations,[31] our assay reliably induces persistent towering within 2 h in 90.4% of trials (292 out of 323 towers), allowing long-term observation and experimental control for reliable quantifications. Continuous monitoring reveals that tower heights largely exhibit steady state during the first 2 h of our assay observation period (Figure S1B [n = 3, CB4856, day 1 adults]). We also observed that worms can tower without a pillar by leaning and climbing on each other (Figure S1C [CB4856, day 1 adults]), although unsupported towers are much rarer, smaller, and transitory (usually 2 mm maximum height and lasting for 10 s, but can be up to 5 mm in height and lasting up to 1 min) compared with pillared towers (11.4 mm maximum height, with 181 out of 233 towers [77.7%] lasting over 12 h). Furthermore, towers growing on slanted pillars as well as both previous[12] and our own field observations (Figures 1A and 1B) suggest that the directionality of towers is guided by substrate orientation rather than gravity. We confirmed this by tilting assay plates at a 90° angle after worm release; towers consistently grew sideways (n = 5), orthogonal to the tilted substrate rather than along the pillar axis (Figure S1D [CB4856, day 1 adults]).

Despite this previously being believed to be a dauer-exclusive behavior,[27] we observed towering in worms from all life stages in both the laboratory reference strain N2 and in the Hawaiian wild isolate CB4856 (Figure 2; Video S2), providing the first evidence that towering could serve as a generalized dispersal behavior. The fact that we have not observed non-dauer towers in the wild may simply be due to limited observations or to yet-unknown factors that invite further investigation. The theoretical generalizability of towering is in contrast to individual nictation, which is characterized by dauer-exclusive molecular factors related to dauer development and neuronal morphology.[17,27,32,33] Indeed, non-dauer towers did not appear to require nictation, as individuals climbed on the pillar or on each other to initiate towering. Interrogating the role of known nictation regulators in the towering behavior of dauer and non-dauer populations will unveil whether towering and nictation are distinct processes. Because all life stages are capable of towering, we also tested for differences in the behavior among life stages and strains. We used a linear mixed-effect model controlling for the effect of pillar length (β = 0.25, confidence interval [CI] = 0.11 to 0.40; t = 3.42) and found that day 1 adults build taller towers than both mixed-stage groups (β = −0.44, CI = −0.70 to −0.17; t = −3.28) and dauers (β = −1.40; CI = −1.80 to −1.00; t = −6.93), which form the shortest towers despite being the main dispersal stage (Figure 2D). Our results potentially suggest a positive effect of body size and movement coordination on the day 1 adult towers and that dauers are perhaps not as compelled to tower together due to their ability to disperse individually[12,13,16,17] and survive long periods.[24,25] We also found that the wild isolate

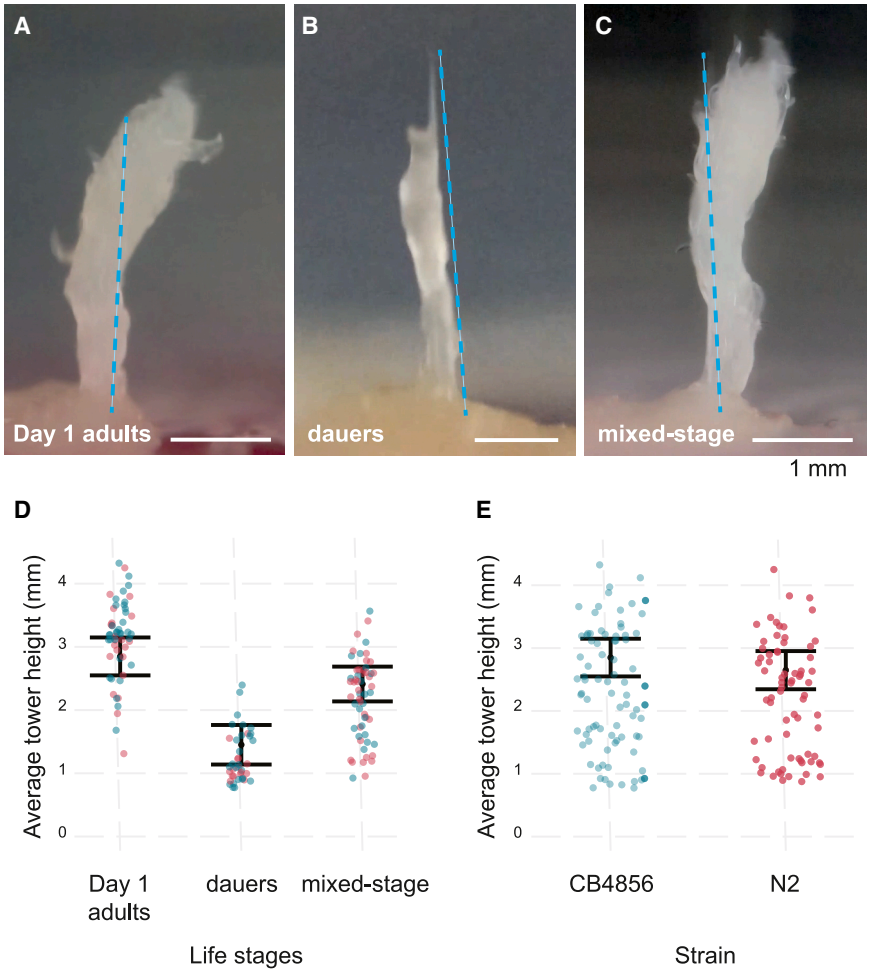

Figure 2. Worms from all life stages can tower

Snapshots from towering assays with populations composed of (A) day 1 adults, (B) dauers, and (C) mixed-stage animals (strain CB4856; blue dashed line: pillar) (Video S2). Distinct (D) life stages and (E) strains present different tower heights. Datapoints represent average tower heights of individual assays (blue: CB4856; pink: N2). Linear mixed-effect model effects and SE are indicated by the bars and model AICs are provided in Table S1. See also Figure S1.

CB4856 builds slightly taller towers than N2 (β = −0.20; CI = −0.35 to −0.05; t = −2.60; Figure 2E), potentially suggesting a role of sociality[34] or enhanced motility[35,36] in the process.

We went on to exploit our lab assay to assess further characteristics of towering behavior. First, we used worms with fluorescently labeled pharynxes to visualize position and orientation within the tower structure at single-worm resolution. We observed considerable alignment of heads and bodies as worms climbed upward away from the substrate (e.g., polar order) (Figure 3A [OMG8, day 1 adults]; Video S3). This is a new feature of worm aggregation, as worm collectives previously reported to form 2D networks on a Petri dish lid show both alignment and anti-alignment (e.g., nematic order),[37] while those aggregating on food in 2D are disordered, without overt alignment.[38] Next, we assessed tower capabilities by growing larger towers (~16,000 worms in the assay plate) on longer pillars (n = 8) and found that towers could greatly surpass the pillar tip (>1 cm). Previous studies have shown that towers can contain thousands of individuals,[15] stand an impressive 5 cm,[12] and can form bridges across gaps.[16] Indeed, our large towers can grow tall with dynamic and coordinated movement of individuals for potential gap crossing and dispersal. They can form an unsupported arm that freely explores the 3D space before collapsing and merging back into the main tower (Figure 3B [CB4856, day 1 adults]; Video S4). If the arm collapsed, worms changed body orientation to re-establish the original alignment, causing temporary disruption and branching to the main tower structure, which soon stabilized and extended into a new exploratory arm (Figure 3B; Video S4). On one occasion, the arm bridged an ~3 mm gap beyond the tip of the pillar to the Petri dish lid above, forming a smooth and stable bridge allowing the transport of worms from the agar surface at the bottom to the lid at the top (Figure 3C [CB4856, day 1 adults]; Video S4). Future investigations tracking the positional dynamics of fluorescently tagged individuals inside the towers could reveal their spatial-temporal organization to achieve structural integrity and sustained growth.

Towers can explore the space to disperse, but which sensory cues are salient for them to respond to? Previous evidence of whole-tower transfer involved electric field sensing for vector attachment,[14] and tactile stimulation with a pick induces attachment in the field (this study, Video S1) and in semi-natural conditions.[13] We touched the top of a lab-grown tower with a glass pick to simulate mechanical cues from potential vectors. The touch instigated tower growth in the direction of the stimulus (Figure 3D [CB4856, mixed stage]; Video S5), culminating in the top segment of the tower attaching to the pick and ~110 individuals simultaneously dispersing to a new, nutrient-rich habitat. The dispersed population consisted of mixed-stage individuals with a qualitatively similar size distribution to that of the starting population in this experiment (Figure 3D; Video S5). The residual tower exhibited renewed growth within 90 s after stimulation, developing multiple apical projections comprising an estimated 2–20 individuals each (Figure 3D; Video S5) that could potentially prepare the tower for subsequent attachment events. The glass pick here is an inert material, suggesting that mechano-sensation alone is sufficient for phoretic collective dispersal, though olfactory, chemo-, or electro-sensing may also play a role. Although a previous study demonstrated that *C. elegans* is generally not attracted to the volatile odorants or secreted compounds from known vectors for this species, including isopods, fruit flies, and

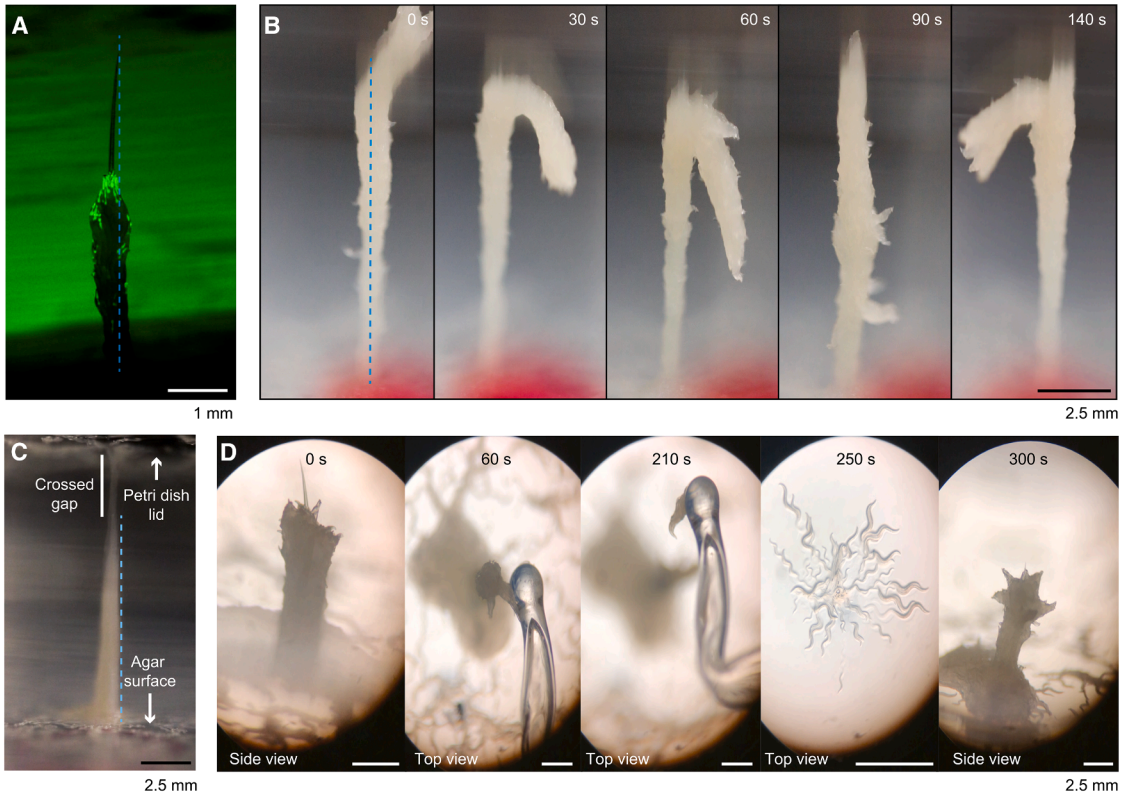

Figure 3. Worm towers are aligned and active self-assemblages that can confer collective dispersal

(A) A tower of worms with GFP-labeled pharynxes (OMG8, day 1 adults; blue dashed line: pillar) (Video S3).

(B) A tower explores the 3D space with an unsupported arm (Video S4) (CB4856, day 1 adults; blue dashed line: pillar).

(C) A tower bridges an ~3 mm gap to reach the Petri dish lid (CB4856, day 1 adults; blue dashed line: pillar) (Video S4).

(D) Touch experiment showing the tower prior to tactile stimulation, active attachment to pick, group transfer, the individuals that transferred, and post-transfer tower re-growth with multi-directional branching (CB4856, mixed-stage population) (Video S5). See also Figure S1.

myriapods,[39,40] the case may be different for nematode species with a narrow vector association, such as *C. japonica* to the burrower bug *Parastrachia japonensis*, fig-associated nematodes to fig pollinating wasps, and many *Pristionchus* spp. to coleopterans, all of which depend on chemical recognition.[41–43] Given the availability of many touch receptor mutants in *C. elegans*, future studies could investigate which receptors are involved in towering to clarify the potential contribution of multiple mechano-sensory pathways involved in different parts of the process (e.g., sensing conspecifics, the vector, and the environment).

The dispersed population from the touch experiment were from the top of the tower, prompting the question of whether there is spatial sorting or role specialization of individuals in the group. Could it be that worms at the top are more fecund, while those at the bottom are physically stronger to support the load? We grew towers with day 1 adults at the beginning of their brood period and collected individuals from these positions as well as non-towering worms from the agar surface. We counted the total number of offspring from single hermaphrodite mothers and found no difference in the total brood size between the three positions (Figure 4A [CB4856, day 1 adults]; $\chi^2 = 2.935$, $p = 0.230$). We also measured the number of lateral body bends (thrash) a worm performs in a droplet of M9 buffer to assess muscular strength[44] and detected no significant differences (Figure 4B [CB4856, day 1 adults]; $\chi^2 = 3.344$, $p = 0.188$). Lastly, we assessed locomotion attributes with a crawling assay. Principal-component analysis (PCA) of 16 quantitative behavioral features reveals that even though worms from outside of the towers show the widest spread, data points from all three tower positions largely cluster together in PC space (Figure 4C [CB4856, day 1 adults]). Our results thus suggest the absence of role specialization and a lack of competition for privileged distal positions in these towers, consistent with our previous observation that the dispersed population from a mixed-stage tower is also mixed (Figure 3D [CB4856, mixed stage]). The lack of competition in clonal *C. elegans* populations is unsurprising; future studies with heterogeneous populations could reveal how genetic composition of the group influences cooperation, competition, and dispersal success.

Given the empirical, behavioral, or taxonomic limitations of other self-assembling collective dispersal systems (e.g., ant towers, spider mite silk balls, and *Dictyostelium* fruiting bodies[5–11]), it is challenging to rigorously interrogate the mechanistic basis of collective dispersal and place this into an evolutionary and ecological context. Our study establishes nematode towering behavior as an excellent system for addressing

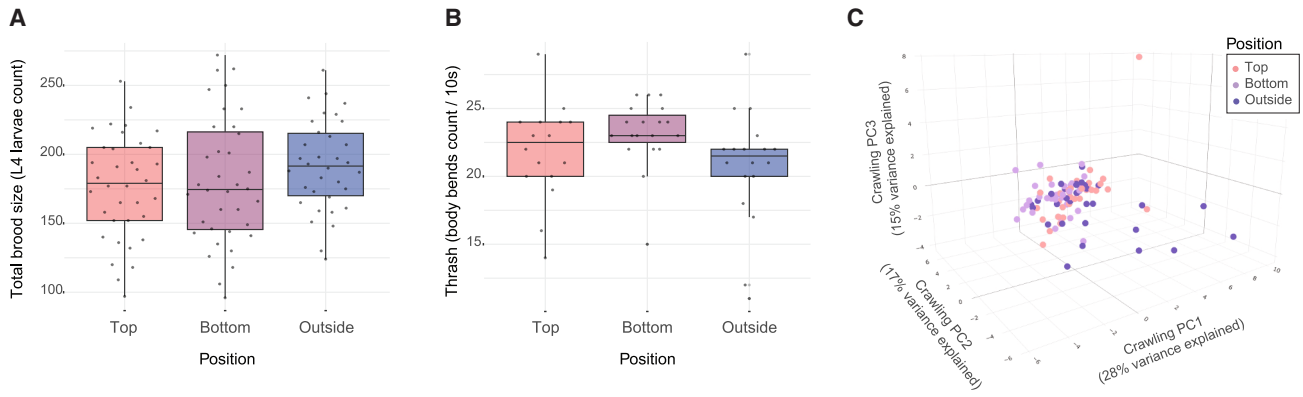

Figure 4. No clear evidence of role specialization in towers

Worms sampled from top and bottom tower positions or from outside the tower showed similar reproductive, physiological, and locomotion conditions (CB4856, day 1 adults).

(A) Boxplot indicating brood sizes across tower positions.

(B) Boxplot indicating body bend counts across different tower positions. Linear mixed-effect models AICs are provided in Table S1.

(C) First three principal components from the PCA of a crawling locomotion assay.

these questions. First, we provided the missing evidence for nematode towers under natural conditions and confirmed the structure's ability to facilitate collective dispersal via phoresy. We then developed a robust laboratory towering assay to characterize and manipulate towering behavior under replicable, standardized conditions. By leveraging the wealth of knowledge, tools, and wild isolates available for *C. elegans*, we have set the stage for characterizing the genetic, organismal, and social mechanisms of collective dispersal. Given the feasibility of applying methods established here for *C. elegans* to both closely and distantly related nematode taxa, comparative studies of towering behavior and its underlying mechanisms among nematode species will yield insights into the intrinsic and extrinsic variables governing patterns of behavioral diversification across the phylum. Thus, nematode towering stands to serve as a fruitful model to elucidate the molecular, ecological, and evolutionary factors governing collective dispersal.

RESOURCE AVAILABILITY

Lead contact

Further information and requests for resources, reagents, or experimental details should be directed to and will be fulfilled by the lead contact, Siyu Serena Ding (serena.ding@ab.mpg.de).

Materials availability

This study did not generate new unique reagents. *C. elegans* strains N2 and CB4856 used in this study are available from the *Caenorhabditis* Genetics Center (CGC); *C. elegans* strain OMG8 was obtained from the laboratory of Andre Brown. Representative wild strains of *C.* sp. 8, *C. remanei*, and *C. elegans* isolated in this study can be made available upon request.

Data and code availability

- The data generated are publicly available at GitHub at https://github.com/SerenaDingLab/Perez_et_al_Towers24.
- The code created to analyze the data is publicly available at GitHub at https://github.com/SerenaDingLab/Perez_et_al_Towers24.
- Any additional information required to reanalyze the data reported in this work paper is available from the lead contact upon request.

ACKNOWLEDGMENTS

We would like to credit Elin Georgiev for granting access to the mushroom farm and sharing long-term observations of nematode populations on the farm. We thank Marie-Anne Félix and Ray Hong for sharing unpublished personal communications on nematode towers. We are grateful for Akhila Mudunuri providing *Drosophila melanogaster* and for Youn Jae Kang helping with imaging GFP worm towers. Some strains were provided by the CGC, which is funded by NIH Office of Research Infrastructure Programs (P40 OD010440). This study was funded through the Max Planck Institute of Animal Behavior and the BABOTs consortium grant (Horizon Europe, European Innovation Council Pathfinder Work Programme under grant agreement no. 101098722) to S.S.D. D.M.P. was supported by a postdoc fellowship from the Alexander von Humboldt Foundation and by the Deutsche Forschungsgemeinschaft (DFG, German Research Foundation) under Germany's Excellence Strategy—EXC 2117 – 422037984—to conduct this research.

AUTHOR CONTRIBUTIONS

D.M.P., T.S., and S.S.D. conceived the study; D.M.P., R.G., T.S., and N.F.-M. carried out the experiments; D.M.P., R.G., T.S., N.F.-M., and A.P. analyzed the data; D.M.P., R.G., T.S., N.F.-M., A.P., and S.S.D. discussed the results and wrote the manuscript; D.M.P. and S.S.D. acquired funding for the project; S. S.D. supervised the project.

DECLARATION OF INTERESTS

The authors declare no competing interests.

STAR★METHODS

Detailed methods are provided in the online version of this paper and include the following:

- KEY RESOURCES TABLE
- EXPERIMENTAL MODEL AND STUDY PARTICIPANT DETAILS
- METHOD DETAILS
  - Field work and species identification
  - Laboratory tower assay
- QUANTIFICATION AND STATISTICAL ANALYSIS
  - Behavioral recording and quantification
  - Statistical analysis

SUPPLEMENTAL INFORMATION

Supplemental information can be found online at https://doi.org/10.1016/j.cub.2025.05.026.

Received: October 10, 2024
Revised: March 10, 2025
Accepted: May 9, 2025
Published: June 5, 2025

REFERENCES

1. Bonte, D., Van Dyck, H., Bullock, J.M., Coulon, A., Delgado, M., Gibbs, M., Lehouck, V., Matthysen, E., Mustin, K., Saastamoinen, M., et al. (2012). Costs of dispersal. Biol. Rev. Camb. Philos. Soc. *87*, 290–312. https://doi.org/10.1111/j.1469-185X.2011.00201.x.
2. Corcobado, G., Rodríguez-Gironés, M.A., Moya-Laraño, J., and Avilés, L. (2012). Sociality level correlates with dispersal ability in spiders. Funct. Ecol. *26*, 794–803. https://doi.org/10.1111/j.1365-2435.2012.01996.x.
3. Cote, J., Bocedi, G., Debeffe, L., Chudzińska, M.E., Weigang, H.C., Dytham, C., Gonzalez, G., Matthysen, E., Travis, J., Baguette, M., et al. (2017). Behavioural synchronization of large-scale animal movements – disperse alone, but migrate together?: Synchronization of large-scale animal movements. Biol. Rev. Camb. Philos. Soc. *92*, 1275–1296. https://doi.org/10.1111/brv.12279.
4. Mazzei, R., and Rubenstein, D.R. (2021). Larval ecology, dispersal, and the evolution of sociality in the sea. Ethology *127*, 808–820. https://doi.org/10.1111/eth.13195.
5. Strassmann, J.E., and Queller, D.C. (2011). Evolution of cooperation and control of cheating in a social microbe. Proc. Natl. Acad. Sci. USA *108*, 10855–10862. https://doi.org/10.1073/pnas.1102451108.
6. Anderson, C., Theraulaz, G., and Deneubourg, J.-L. (2002). Self-assemblages in insect societies. Insectes Soc. *49*, 99–110. https://doi.org/10.1007/s00040-002-8286-y.
7. Clotuche, G., Mailleux, A.-C., Astudillo Fernández, A., Deneubourg, J.-L., Detrain, C., and Hance, T. (2011). The Formation of Collective Silk Balls in the Spider Mite Tetranychus urticae Koch. PLOS One *6*, e18854. https://doi.org/10.1371/journal.pone.0018854.
8. Clotuche, G., Navajas, M., Mailleux, A.-C., and Hance, T. (2013). Reaching the Ball or Missing the Flight? Collective Dispersal in the Two-Spotted Spider Mite Tetranychus urticae. PLOS One *8*, e77573. https://doi.org/10.1371/journal.pone.0077573.
9. Foster, P.C., Mlot, N.J., Lin, A., and Hu, D.L. (2014). Fire ants actively control spacing and orientation within self-assemblages. J. Exp. Biol. *217*, 2089–2100. https://doi.org/10.1242/jeb.093021.
10. Phonekeo, S., Mlot, N., Monaenkova, D., Hu, D.L., and Tovey, C. (2017). Fire ants perpetually rebuild sinking towers. R. Soc. Open Sci. *4*, 170475. https://doi.org/10.1098/rsos.170475.
11. Smith, J., Queller, D.C., and Strassmann, J.E. (2014). Fruiting bodies of the social amoeba Dictyostelium discoideum increase spore transport by Drosophila. BMC Evol. Biol. *14*, 105. https://doi.org/10.1186/1471-2148-14-105.
12. Hesling, J.J. (1966). Preliminary experiments on the control of mycophagous eelworms in mushroom beds, with a note on their swarming. Plant Pathol. *15*, 163–166. https://doi.org/10.1111/j.1365-3059.1966.tb00342.x.
13. Staniland, L.N. (1957). The swarming of Rhabditid eelworms in mushroom houses. Plant Pathol. *6*, 61–62. https://doi.org/10.1111/j.1365-3059.1957.tb00775.x.
14. Chiba, T., Okumura, E., Nishigami, Y., Nakagaki, T., Sugi, T., and Sato, K. (2023). Caenorhabditis elegans transfers across a gap under an electric field as dispersal behavior. Curr. Biol. *33*, 2668–2677.e3. https://doi.org/10.1016/j.cub.2023.05.042.
15. Félix, M.-A., and Duveau, F. (2012). Population dynamics and habitat sharing of natural populations of Caenorhabditis elegans and C. briggsae. BMC Biol. *10*, 59. https://doi.org/10.1186/1741-7007-10-59.
16. Penkov, S., Ogawa, A., Schmidt, U., Tate, D., Zagoriy, V., Boland, S., Gruner, M., Vorkel, D., Verbavatz, J.-M., Sommer, R.J., et al. (2014). A wax ester promotes collective host finding in the nematode Pristionchus pacificus. Nat. Chem. Biol. *10*, 281–285. https://doi.org/10.1038/nchembio.1460.
17. Lee, H., Choi, M.K., Lee, D., Kim, H.S., Hwang, H., Kim, H., Park, S., Paik, Y.K., and Lee, J. (2011). Nictation, a dispersal behavior of the nematode Caenorhabditis elegans, is regulated by IL2 neurons. Nat. Neurosci. *15*, 107–112. https://doi.org/10.1038/nn.2975.
18. Félix, M.-A., and Braendle, C. (2010). The natural history of Caenorhabditis elegans. Curr. Biol. *20*, R965–R969. https://doi.org/10.1016/j.cub.2010.09.050.
19. Grewal, P.S. (1991). Effects of *Caenorhabditis elegans* (Nematoda: Rhabditidae) on the spread of the bacterium *Pseudomonas tolaasii* in mushrooms (*Agaricus bisporus*). Ann. Appl. Biol. *118*, 47–55. https://doi.org/10.1111/j.1744-7348.1991.tb06084.x.
20. Venette, R.C., and Ferris, H. (1998). Influence of bacterial type and density on population growth of bacterial-feeding nematodes. Soil Biol. Biochem. *30*, 949–960. https://doi.org/10.1016/S0038-0717(97)00176-4.
21. Frézal, L., and Félix, M.-A. (2015). C. elegans outside the Petri dish. eLife *4*, e05849. https://doi.org/10.7554/eLife.05849.
22. Kiontke, K.C., Félix, M.-A., Ailion, M., Rockman, M.V., Braendle, C., Pénigault, J.-B., and Fitch, D.H.A. (2011). A phylogeny and molecular barcodes for Caenorhabditis, with numerous new species from rotting fruits. BMC Evol. Biol. *11*, 339. https://doi.org/10.1186/1471-2148-11-339.
23. Sloat, S.A., Noble, L.M., Paaby, A.B., Bernstein, M., Chang, A., Kaur, T., Yuen, J., Tintori, S.C., Jackson, J.L., Martel, A., et al. (2022). *Caenorhabditis* nematodes colonize ephemeral resource patches in neotropical forests. Ecol. Evol. *12*, e9124. https://doi.org/10.1002/ece3.9124.
24. Crook, M. (2014). The dauer hypothesis and the evolution of parasitism: 20 years on and still going strong. Int. J. Parasitol. *44*, 1–8. https://doi.org/10.1016/j.ijpara.2013.08.004.
25. Corsi, A.K., Wightman, B., and Chalfie, M. (2015). A Transparent Window into Biology: A Primer on *Caenorhabditis elegans*. Genetics *200*, 387–407. https://doi.org/10.1534/genetics.115.176099.
26. Guisnet, A., Maitra, M., Pradhan, S., and Hendricks, M. (2021). A three-dimensional habitat for C. elegans environmental enrichment. PLOS One *16*, e0245139. https://doi.org/10.1371/journal.pone.0245139.
27. Yang, H., Lee, B.Y., Yim, H., and Lee, J. (2020). Neurogenetics of nictation, a dispersal strategy in nematodes. J. Neurogenet. *34*, 510–517. https://doi.org/10.1080/01677063.2020.1788552.
28. Cutter, A.D. (2006). Nucleotide Polymorphism and Linkage Disequilibrium in Wild Populations of the Partial Selfer *Caenorhabditis elegans*. Genetics *172*, 171–184. https://doi.org/10.1534/genetics.105.048207.
29. Sudhaus, W., Giblin-Davis, R., and Kiontke, K. (2011). Description of Caenorhabditis angaria n. sp. (Nematoda: Rhabditidae), an associate of sugarcane and palm weevils (Coleoptera: Curculionidae). Nematol. *13*, 61–78. https://doi.org/10.1163/138855410X500334.
30. Kiontke, K. (1997). Description of Rhabditis (Caenorhabditis) drosophilae n. sp. and R. (C.) sonorae n. sp. (Nematoda : Rhabditida) from saguaro cactus rot in Arizona. Fundam. Appl. Nematol. *20*, 305–315.
31. Tanaka, R., Okumura, E., and Yoshiga, T. (2010). A simple method to collect phoretically active dauer larvae of Caenorhabditis japonica. Jpn. J. Nematol. *40*, 7–12. https://doi.org/10.3725/jjn.40.7.
32. Schroeder, N.E., Androwski, R.J., Rashid, A., Lee, H., Lee, J., and Barr, M.M. (2013). Dauer-Specific Dendrite Arborization in C. elegans Is Regulated by KPC-1/Furin. Curr. Biol. *23*, 1527–1535. https://doi.org/10.1016/j.cub.2013.06.058.

33. Lee, D., Yang, H., Kim, J., Brady, S., Zdraljevic, S., Zamanian, M., Kim, H., Paik, Y.K., Kruglyak, L., Andersen, E.C., et al. (2017). The genetic basis of natural variation in a phoretic behavior. Nat. Commun. *8*, 273. https://doi.org/10.1038/s41467-017-00386-x.

34. De Bono, M., and Bargmann, C.I. (1998). Natural Variation in a Neuropeptide Y Receptor Homolog Modifies Social Behavior and Food Response in C. elegans. Cell *94*, 679–689. https://doi.org/10.1016/S0092-8674(00)81609-8.

35. Helms, S.J., Rozemuller, W.M., Costa, A.C., Avery, L., Stephens, G.J., and Shimizu, T.S. (2019). Modelling the ballistic-to-diffusive transition in nematode motility reveals variation in exploratory behaviour across species. J. R. Soc. Interface *16*, 20190174. https://doi.org/10.1098/rsif.2019.0174.

36. Bendesky, A., Tsunozaki, M., Rockman, M.V., Kruglyak, L., and Bargmann, C.I. (2011). Catecholamine receptor polymorphisms affect decision-making in C. elegans. Nature *472*, 313–318. https://doi.org/10.1038/nature09821.

37. Sugi, T., Ito, H., Nishimura, M., and Nagai, K.H. (2019). C. elegans collectively forms dynamical networks. Nat. Commun. *10*, 683. https://doi.org/10.1038/s41467-019-08537-y.

38. Ding, S.S., Schumacher, L.J., Javer, A.E., Endres, R.G., and Brown, A.E. (2019). Shared behavioral mechanisms underlie C. elegans aggregation and swarming. eLife *8*, e43318. https://doi.org/10.7554/eLife.43318.

39. Petersen, C., Krahn, A., and Leippe, M. (2023). The nematode Caenorhabditis elegans and diverse potential invertebrate vectors predominantly interact opportunistically. Front. Ecol. Evol. *11*, 1069056. https://doi.org/10.3389/fevo.2023.1069056.

40. Archer, H., Deiparine, S., and Andersen, E.C. (2020). The nematode Caenorhabditis elegans and the terrestrial isopod Porcellio scaber likely interact opportunistically. PLOS One *15*, e0235000. https://doi.org/10.1371/journal.pone.0235000.

41. Okumura, E., and Yoshiga, T. (2014). Host orientation using volatiles in the phoretic nematode Caenorhabditis japonica. J. Exp. Biol. Jeb, 105353. https://doi.org/10.1242/jeb.105353.

42. Krishnan, A., Muralidharan, S., Sharma, L., and Borges, R.M. (2010). A hitchhiker's guide to a crowded syconium: how do fig nematodes find the right ride? Funct. Ecol. *24*, 741–749. https://doi.org/10.1111/j.1365-2435.2010.01696.x.

43. Hong, R.L., and Sommer, R.J. (2006). Chemoattraction in Pristionchus Nematodes and Implications for Insect Recognition. Curr. Biol. *16*, 2359–2365. https://doi.org/10.1016/j.cub.2006.10.031.

44. Miller, K.G., Alfonso, A., Nguyen, M., Crowell, J.A., Johnson, C.D., and Rand, J.B. (1996). A genetic selection for Caenorhabditis elegans synaptic transmission mutants. Proc. Natl. Acad. Sci. USA *93*, 12593–12598. https://doi.org/10.1073/pnas.93.22.12593.

45. Holterman, M., Van Der Wurff, A., Van Den Elsen, S., Van Megen, H., Bongers, T., Holovachov, O., Bakker, J., and Helder, J. (2006). Phylum-Wide Analysis of SSU rDNA Reveals Deep Phylogenetic Relationships among Nematodes and Accelerated Evolution toward Crown Clades. Mol. Biol. Evol. *23*, 1792–1800. https://doi.org/10.1093/molbev/msl044.

46. Schneider, C.A., Rasband, W.S., and Eliceiri, K.W. (2012). NIH Image to ImageJ: 25 years of image analysis. Nat. Methods *9*, 671–675. https://doi.org/10.1038/nmeth.2089.

47. Javer, A., Currie, M., Lee, C.W., Hokanson, J., Li, K., Martineau, C.N., Yemini, E., Grundy, L.J., Li, C., Ch'ng, Q., et al. (2018). An open-source platform for analyzing and sharing worm-behavior data. Ch. Nat. Methods *15*, 645–646. https://doi.org/10.1038/s41592-018-0112-1.

48. Bates, D., Mächler, M., Bolker, B., and Walker, S. (2015). Fitting Linear Mixed-Effects Models Using **lme4**. J. Stat. Soft. *67*. https://doi.org/10.18637/jss.v067.i01.

49. Bolker, B., and R Development Core Team. (2007). bbmle: Tools for General Maximum Likelihood Estimation. https://doi.org/10.32614/CRAN.package.bbmle.

50. Lüdecke, D., Ben-Shachar, M., Patil, I., Waggoner, P., and Makowski, D. (2021). performance: An R Package for Assessment, Comparison and Testing of Statistical Models. JOSS *6*, 3139. https://doi.org/10.21105/joss.03139.

51. Hartig, F. (2016). DHARMa: Residual Diagnostics for Hierarchical (Multi-Level/Mixed) Regression Models. https://doi.org/10.32614/CRAN.package.DHARMa.

52. Fox, J., Weisberg, S., and Price, B. (2019). An R Companion to applied regression. 3.1–3.

53. Wickham, H. (2016). Getting Started with ggplot2. In ggplot2 Use R! (Springer International Publishing), pp. 11–31. https://doi.org/10.1007/978-3-319-24277-4_2.

54. Sievert, C., Parmer, C., Hocking, T., Chamberlain, S., Ram, K., Corvellec, M., and Despouy, P. (2024). plotly: Create Interactive Web Graphics via "plotly.js.". https://doi.org/10.32614/CRAN.package.plotly.

55. Bauer, D.J., and Curran, P.J. (2005). Probing Interactions in Fixed and Multilevel Regression: Inferential and Graphical Techniques. Multivariate Behav. Res. *40*, 373–400. https://doi.org/10.1207/s15327906mbr4003_5.

56. Barrière, A., and Félix, M.A. (2006). Isolation of C. elegans and related nematodes. Book. WormBook, 1–9. https://doi.org/10.1895/wormbook.1.115.1.

57. Lissemore, J.L., Lackner, L.L., Fedoriw, G.D., and De Stasio, E.A. (2005). Isolation of *Caenorhabditis elegans* genomic DNA and detection of deletions in the *unc-93* gene using PCR. Biochem. Mol. Biol. Educ. *33*, 219–226. https://doi.org/10.1002/bmb.2005.494033032452.

58. Fay, D., and Bender, A. (2006). Genetic mapping and manipulation: Chapter 4-SNPs: Introduction and two-point mapping. WormBook, pp 1–7. https://doi.org/10.1895/wormbook.1.93.1.

59. Camacho, C., Coulouris, G., Avagyan, V., Ma, N., Papadopoulos, J., Bealer, K., and Madden, T.L. (2009). BLAST+: architecture and applications. BMC Bioinfo *10*, 421. https://doi.org/10.1186/1471-2105-10-421.

60. Barlow, I.L., Feriani, L., Minga, E., McDermott-Rouse, A., O'Brien, T.J., Liu, Z., Hofbauer, M., Stowers, J.R., Andersen, E.C., Ding, S.S., et al. (2022). Megapixel camera arrays enable high-resolution animal tracking in multiwell plates. Commun. Biol. *5*, 253. https://doi.org/10.1038/s42003-022-03206-1.

61. Javer, A., Ripoll-Sánchez, L., and Brown, A.E.X. (2018). Powerful and interpretable behavioural features for quantitative phenotyping of *Caenorhabditis elegans*. Philos. Trans. R. Soc. Lond. B Biol. Sci. *373*, 20170375. https://doi.org/10.1098/rstb.2017.0375.

62. Pedregosa, F., Varoquaux, G., Gramfort, A., Michel, V., Thirion, B., Grisel, O., Blondel, M., Prettenhofer, P., Weiss, R., Dubourg, V., et al. (2011). Scikit-learn: Machine Learning in Python. Mach. Learn. 2825–2830.

STAR★METHODS

KEY RESOURCES TABLE

REAGENT or RESOURCE	SOURCE	IDENTIFIER
Bacterial and virus strains		
Escherichia coli	CGC	OP50; RRID: WB-STRAIN: WBStrain00041969
Deposited data		
Dataset and code used in the study	This paper. Data were deposited at GitHub	https://github.com/SerenaDingLab/Perez_et_al_Towers24
Experimental models: Organisms/strains		
Caenorhabditis sp. 8	This paper	N/A
Caenorhabditis remanei	This paper	N/A
Caenorhabditis elegans	CGC	N2; RRID: WB-STRAIN:WBStrain00000001
Caenorhabditis elegans	CGC	CB4856; RRID: WB-STRAIN: WBStrain00004602
Caenorhabditis elegans	Andre Brown lab	OMG8
Oligonucleotides		
5′-ctcaaagattaagccatgc-3′	Holterman et al.[45]	988F
5′-tttacggtcagaactaggg-3′	Holterman et al.[45]	1912R
5′-ctgcgtgagaggtgaaat-3′	Holterman et al.[45]	1813F
5′-gctaccttgttacgactttt-3′	Holterman et al.[45]	2646R
Software and algorithms		
ImageJ 1.53t	Schneider et al.[46]	https://imagej.net/ij/
Tierpsy Tracker	Javer et al.[47]	https://github.com/ver228/tierpsy-tracker
R	R Core Team 2024	https://www.r-project.org/
R package *stats*	R Core Team 2024	https://www.r-project.org/
R package *lme4*	Bates et al.[48]	https://cran.r-project.org/web/packages/lme4/index.html
R package *bbmle*	Bolker and R Development Core Team[49]	https://cran.r-project.org/web/packages/bbmle/index.html
R package *performance*	Lüdecke et al.[50]	https://cran.r-project.org/web/packages/performance/index.html
R package *DHARMa*	Hartig[51]	https://cran.r-project.org/web/packages/DHARMa/index.html
R package *car*	Fox et al.[52]	https://cran.r-project.org/web/packages/car/index.html
R package *ggplot2*	Wickham et al.[53]	https://cran.r-project.org/web/packages/ggplot2/index.html
R package *plotly*	Sievert et al.[54]	https://cran.r-project.org/web/packages/plotly/citation.html
R package *interactions*	Bauer & Curran[55]	https://cran.r-project.org/web/packages/interactions/index.html
Other		
Toothbrush	Bevola	Super soft performance sensitive
Field digital microscope	AD246S-M, Andonstar Technology Co.	https://andonstar.com/product/ad246s-m-ad249s-m-3-lenses-10-7-in-lcd-hdmi-digital-microscope/
DSLR camera (EOS 80D) and a macro lens (MP-E 65mmf/2.8 1–5 x)	Canon	https://www.canon.de/for_home/product_finder/cameras/digital_slr/eos-80d/

(*Continued on next page*)

Continued

REAGENT or RESOURCE	SOURCE	IDENTIFIER
Axiozoom V16 upright fluorescence microscope, equipped with an AxioCam 712 color camera and an Illuminator HXP 200C light source	Zeiss	https://www.zeiss.com/microscopy/de/produkte/lichtmikroskope/stereo–und-zoom-mikroskope/axio-zoom-v16-fuer-die-biologie.html

EXPERIMENTAL MODEL AND STUDY PARTICIPANT DETAILS

Nematodes were collected from the University of Konstanz campus orchard (Germany) and a mushroom farm in North Berwick (United Kingdom), and identified based on molecular barcoding of 18S rDNA sequences according to protocols outlined in Barrière and Félix[56] and described below, identifying an undescribed *Caenorhabditis* species (*C*. sp. 8[22,23]), *C. remanei*, and *C. elegans*. Laboratory *C. elegans* strains used in the study included N2 (laboratory reference strain; source: *Caenorhabditis* Genetics Center [CGC]), CB4856 (Hawaiian wild isolate; source: CGC), and OMG8 (*mIs12[myo-2p::GFP + pes-10p::GFP + F22B7.9p::GFP] II* introgressed 10x into CB4856 background; source: Andre Brown lab). All *C. elegans* were cultured on 9 cm NGM plates seeded with 1.5 mL of *E. coli* OP50 culture grown overnight at 37°C (OD_{600} = 2.2; source: CGC), and preparations and behavioral experiments conducted in the laboratory at 20C.

METHOD DETAILS

Field work and species identification

Sediment samples were randomly sampled from mushroom growth flats and plated on 55 mm petri dishes filled with Nematode Growth Media (NGM; 3 g NaCl, 17 g agar, 2.5 g peptone, 972 mL H_2O, 1 mL $CaCl_2$, 1 mL cholesterol [5 mg/mL cholesterol in EtOH], 1 mL $MgSO_4$, 25 mL 1 M KPO_4 buffer pH 6.0) seeded with *E. coli* OP50. A random subset of individual worms that crawled onto the OP50 lawn were picked and transferred to 50 μL RNAlater™ (Invitrogen, USA) for preservation. The plates were then sealed with Parafilm ® (Bemis Company, USA) and transported to the University of Konstanz. We were not able to collect the towers from the mushroom farms to ascertain the exact species composition and animal stages; the collected soil samples consisted mostly of dauer animals by direct observation. Individual nematodes were randomly picked and plated to create isoworm lines. From these preserved samples and isoworm lines, either single worms (preserved samples) or 3-5 pooled individuals (lines) were placed into 3 or 6 μL 1X worm lysis buffer (50 mM KCl, 10 mM Tris-HCl pH 8.3, 2.5 mM $MgCl_2$, 0.45% IGEPAL, 0.45% Tween 20, 0.01% gelatin, with proteinase K added to a final concentration of 0.2 mg/mL) in microcentrifuge tubes for DNA extraction. From rotting fruit samples at the University of Konstanz orchard, towers were picked from the fruit using a digital microscope (AD246S-M, Andonstar Technology Co., China) and platinum wire in the field, subsequently plated in 55 mm petri dishes containing NGM seeded with OP50, sealed with Parafilm ®, and transported to the lab. The entire fruit was then collected in sterile Whirl-Pak® bags (Filtration Group, USA) for transport to the lab. Upon arriving at the lab, the life stage and number of individuals from each tower was determined. A representative subset of individual worms from the plated towers were then picked and placed directly into 1X worm lysis buffer. To characterize the nematode community of the whole fruit, a ∼5-15 g subsample of fruit was placed on a 90 mm petri dish filled with NGM and seeded with a 100 μL of OP50 in the center. After 24-72 hours, individual worms chosen to represent the morphological diversity of observed nematodes were picked from this plated sample and placed in 1X worm lysis buffer. All samples in lysis buffer were frozen at -80° C for at least 10 minutes to crack the cuticle.[57] After freezing, samples were lysed by incubation at 65° C for 60 minutes, followed by 30 minutes at 95° C for heat deactivation of proteinase K.[58] Primer pairs 988F-1912R and 1813F-2646R were used to separately amplify two fragments of the 18S rDNA gene using the conditions optimized for these primers in Holterman et al.,[45] with a final volume of 50 μL, containing 1 μL DNA lysate, 1 μL forward PCR primer, 1 μL reverse PCR primer, 1 μL dNTPs (Qiagen, Germany), 5 μL *Taq* Buffer (New England Biolabs, USA), 0.25 μL Taq polymerase (New England Biolabs, USA), and 40.75 μL H_2O. Amplicons were purified using the Exo-CIP Rapid PCR Cleanup Kit (New England Biolabs, USA), DNA concentration quantified on Qubit using the 1x dsDNA High Sensitivity kit (Invitrogen, USA), and sent to Eurofins Genomics for Sanger sequencing. Sequences received from Eurofins were uniformly trimmed based on chromatogram traces, trimming the first 50 bp from the 5' end of each sequence, and trimming the 3' end to achieve a total length of 850 bp for 988F-1912R and 750 bp for 1813F-2646R. Some sequences required additional trimming of the 5' end, as indicated in Table S2, due to low quality base calling. Trimmed sequences were BLASTed against the NCBI sequence database for Nematoda (taxid:6231) using blastn.[59] Species placement was determined by E value and sequence similarity between the query sequence and top hits from BLAST, with the first hit for each query sequence reported in Table S2. After initial sequencing results confirmed the identity of *C*. sp. 8 and *C. remanei* in 20 towers, we were able to assign all subsequent towering individuals to their respective species based on morphological and behavioral characteristics (male tail morphology, reproductive mode, mating behavior). While it may be possible that females of additional *Caenorhabditis* species could go undetected with this approach, we are confident in our assessment of the single species identity of the towers based on never finding a second species within a single tower in the subset of individuals sequenced across all observations, and never observing males of other *Caenorhabditis* species in a tower dominated by either *C*. sp. 8 or *C. remanei*, despite their presence on the same fruit.

Laboratory tower assay

To obtain the worms for towering assays, stocks for *C. elegans* strains were grown to obtain plates full of gravid hermaphrodites. The worms were washed from plates with M9 buffer (Na_2HPO_4 3 g, KH_2PO_4 6 g, NaCl 5 g, $MgSO_4$ at 1M 1 mL, sterile water 999 mL) and dispensed in falcon tubes to be centrifuged (Centrifuge 5702, Eppendorf) at 1500 rpm for 2 minutes. The supernatant containing OP50 was discarded and more M9 was added to the tube, and this process was repeated two more times. Next, 4mL of bleach (sodium hypochlorite + 5% active chlorine 1.6 mL, NaOH at 1M 1 mL, sterile water 1.4 mL) and 4 mL of M9 was added to each tube. The tubes were vigorously vortexed for 4 minutes to break the worm cuticle and isolate the eggs. M9 was then added to the tubes, the tubes were centrifuged at 2500 rpm for 2 minutes and the supernatant discarded, a process repeated for 5 times until the solution became bleach-free. The tubes were placed in a drum rotator (Disc/Drum Rotator SB2, Stuart) rotating at speed 1 to allow for the eggs to hatch and enter L1 diapause overnight in M9 to achieve a synchronized population. L1 larvae density in M9 was estimated by counting the number of individuals in a 5 μL droplet, and the following procedures were performed to obtain distinct worm populations for behavioral assays. Synchronized Day 1 adult populations were obtained by plating 4000 L1 larvae on a 9 cm NGM plate seeded with exactly 1.5 mL OP50 (OD_{600}=2.2), and waiting ∼56 hours for the larvae to grow into young adults. Dauer populations were obtained by plating 40000 L1 larvae on a 9 cm NGM plate seeded with exactly 1.5 mL OP50 (OD_{600}=2.2) and waiting ∼48 hours for these larvae to reach the L2 stage, starve, and form dauers; the precise amount of OP50 is essential here such that the 40000 larvae could reach L2 and then immediately starve for dauer induction. Mixed-stage populations were obtained by plating 100 L1 larvae on seeded 9 cm NGM plates and passaging for at least three generations by chunking, until a final population of ∼4000 mixed-stage animals was obtained. Worm populations were harvested from stock plates with M9 buffer and the worm solution was transferred to a 15 mL tube. Bacteria was removed through a series of four M9 washes by filling the tube with M9, centrifuging (Centrifuge 5702, Eppendorf) the tube at 1500 rpm for 2 minutes to pellet the worms, and then discarding the supernatant containing the OP50. After four washes the concentrated worm pellet at the bottom of the tube was bacteria-free, thus achieving the starvation condition.

To promote worm towers in the lab, assay plates were prepared by filling each 35 mm Petri dish with ∼3 mL of 2% agar, and planting a toothbrush bristle (Super soft performance sensitive, Bevola) as the climbing pillar ∼0.5 cm away from the plate edge using eyebrow tweezers. The concentrated worm pellet was transferred to the base of the pillar using a glass pipette. Approximately 4000 (± 1000) (∼16,000 for large tower experiments) worms were used in the assays, although the number of worms transferred was not strictly controlled. The worm droplet was left to dry undisturbed for one hour with the petri dish lid off inside a fume hood (Prutscher) at maximum fan capacity setting, during which time the worms formed an aggregate at the base of the pillar and started towering. Different pillar materials were tested during the development of this laboratory tower assay before finalizing on the toothbrush bristle. We found that worms could not climb pillars made out of glass due to a lack of friction, and pillars made from animal hair and platinum wire led to desiccation and animal death. Plant thorn, ginger scaffold, apple scaffold and cotton threads have too high friction leading to single worms frequently climbing individually rather than towering together; plus, these materials also lack experimental standardization and so were eventually discarded in favor of toothbrush bristle for this assay.

QUANTIFICATION AND STATISTICAL ANALYSIS

Behavioral recording and quantification

Various techniques were employed to image the towers. Imaging of natural towers was performed using a digital microscope (AD246S-M, Andonstar Technology Co., China) with the 18-720x "Lens A" objective, mounted on a rotating boom arm to enable positioning above the fruits with minimal disturbance at the University of Konstanz orchard. The same imaging set up was used in the lab for observing the behavior continuously for long periods (>4 hours) (Figures 1A, 1C, and S1B). Towers were also imaged with a DSLR camera (Canon EOS 80D) and a macro lens (Canon Macro Lens MP-E 65mmf/2.8 1-5 x, Canon) on the mushroom farm in North Berwick (Figure 1B). To image lab-produced towers, side view footage was captured with the DSLR camera and macro lens set to magnification 3 to 4x (Figures 2A–2C) or to 1x (Figures 3B and 3C), with enough field of view to capture tower morphology. Additional qualitative imaging of towers in the lab was conducted using a phone camera (iPhone 12 Pro, Apple) through the ocular of a dissecting microscope (Stemi 508, Zeiss) using a phone camera adaptor (LabCam for iPhone, Ilabcam) (Figure 3D). To image individual GFP-labeled worms inside towers (Figure 3A), the assay plate was tilted at 90 degrees under the Axio Zoom V16 (Zeiss) upright fluorescence microscope equipped with an AxioCam 712 color camera (Zeiss; Illuminator HXP 200C light source, excitation filter 450-490 nm, emission filter 500-550 nm). Images were acquired at 23 frames per second.

For quantification, the bare pillars without worms were imaged next to a caliper for scale prior to the experiment. The software ImageJ 1.53t[46] was used to measure pillar length and tower height from the recorded towers. Average tower height was measured from three frames with an hourly inter-frame interval for subsequent statistical analysis. This sampling frequency was sufficient because tower heights roughly exhibit steady-state during the first two hours of our assay, as verified by bespoke automated tower tracking and time series analysis of tower heights from 4-hour continuous video recordings (Figure S1B). We tracked towers and assessed tower heights over time using a MATLAB script. First, the tower bases were annotated manually, and a rectangular Region of Interest was defined—centered on each base's y-coordinate and sized to fully encompass the tower. Then one frame per second was sampled and each pair of consecutive frames were compared to compute the absolute difference between them. A brightness

threshold was applied to identify pixels showing significant change, and the highest vertical coordinate among these pixels was recorded as the tower height. Verification videos were generated, and dynamic regions were manually inspected to ensure the quality and consistency of the measurements.

To test for role specialization among individuals within the tower, we conducted brood size, thrash and crawling assays. For brood size assay, a single Day 1 adult at the beginning of their brood period was collected from the top, the bottom, or outside of a given tower for the brood size assay (n = 36). This was done by carefully picking off the whole tower with tweezers and laying it flat on an unseeded plate to let worms crawl out of the tower pillar, so that one worm from the top and one from the bottom could be isolated and collected. The worm from outside the tower was picked directly from the agar surface of the assay plate. The worms were individually transferred to a well of a standard six-well plate filled with 3 mL of no-peptone NGM agar seeded with 60 μL of OP50 for 24 hours to lay eggs. Each worm was transferred to a new well every 24 hours to avoid crowding and overlapping generations in the well, and this was repeated four times to cover the entire brood period. All multi-well plates containing the eggs were stored until the offspring reached L4 to adult stage for counting of the total brood size. For thrash assay in liquid, one worm each was picked from the top, the bottom, or outside of a given tower as described above (n = 19). Each picked individual was transferred into a 100 μL droplet of M9 in a watch glass plate, habituated for 10 seconds, and its thrashing movements were recorded for 10 seconds at 30 frames per second using the phone camera attached to the microscope ocular. The videos were scored manually for the number of times the worm laterally bent its body into a C-shape during those 10 recorded seconds. For crawling assay on agar, one worm each was picked from the top, the bottom, or outside of a given tower as described above (n = 32). Each picked individual was transferred to an individual well of a standard six-well plate filled with 3 mL of no-peptone NGM agar (NaCl 3g, agar 17g, $CaCl_2$ [1M] 1 mL, $MgSO_4$ [1M] 1 mL, KPO_4 buffer [pH 6.0 at 1M] 25 mL, cholesterol [5 mg/mL in EtOH] 1 mL, sterile water 972 mL) seeded with 60 μL of OP50. Worms were habituated for 5 minutes and recorded for 10 minutes at 25 Hz using the commercially available Kastl high-throughput megapixel camera array imaging system[60] (Loopbio GmbH). To analyze the crawling behavior, recorded videos were run through Tierpsy Tracker software to automatically extract a set of 16 quantitative behavioral features[47,61] for each recorded individual. Missing values (NaN) from the feature matrix were imputed with the mean value for each feature column, and the resultant feature matrix was z-normalized. Using Python, a PCA was conducted on the transformed feature matrix using the built-in PCA function from the Scikit-learn Python package.[62]

Statistical analysis

All statistical tests were performed in R (v. 4.3.3) (R Core Team 2024) in RStudio (v. 2023.12.1+402) with the significance level set at $\alpha = 0.05$. To test the effect of food on tower height, a linear regression model (LM) using *lm* function from *stats* package was run using experiments with CB4856 Day 1 adults with (n = 11) or without (n = 12) OP50 in the assay plate (Figure S1A). Tower height was pitted as the response variable, with the type of plate (presence or absence of food) as a fixed explanatory variable. To test the effect of life stages and strain on towering (Figure 2), a linear mixed-effect model (LMM) using the *lmer* function from *lme4* package[48] was fit with mean tower height as the response variable. We used strain (N2 or CB4856) and life stage (Day 1 adult, dauer, or mixed-stage) as fixed explanatory variables (n = 153), pillar length (filtered to a range between 2 and 4 mm) as a covariate, and assay date as a random effect. The final minimal adequate model for tower average height contains all covariates (strain, life stage and pillar length) and had substantial explanatory power (conditional R^2 = 0.73), as did our fixed effects alone (marginal R^2 = 0.57). Standardized parameters were obtained by fitting the model on a standardized version of the dataset, while confidence intervals were computed using a Wald t-distribution approximation. To test whether worms from the top, the bottom, or outside the tower had reproductive condition differences (Figure 4A), a LMM was run using total brood size as response variable and worm position (three levels: top, bottom or outside) and tower height as fixed explanatory variables. To assess the effect of physiological conditions (Figure 4B), a LMM was run using thrash counts (z-transformed) as response variable. Position (three levels: top, bottom or outside) and tower height were pitted as fixed explanatory variables. The effect of pillar length was not included in the model, since towers were picked as soon as they reached the top of the pillar so pillar length was equivalent to tower height. Plate ID (three worms picked from each plate) was accounted for in all models as a random factor. To obtain the simplest model with a minimum of predictors that explains the maximum variance, model selection was performed by starting with the full model structure with all predictors, and then dropping the variables one by one and assessing the effect compared to the full model using the Akaike Information Criterion (AIC) (AICtab in the *bbmle*[49]) and χ^2 tests (*anova* function in the *car* package[52]). Response variable frequency distributions were checked for normality and data transformations were conducted when necessary. All assumptions for model fit were visually inspected for e.g. residuals distribution using the packages *DHARMa*[51] and *performance*.[50] The model results and raw data were plotted using the packages *ggplot2*[53] *plotly*[54] *interactions*.[55]